The 8th European Congress on Computational Methods in Applied Sciences and Engineering
ECCOMAS Congress 2022
5 – 9 June 2022, Oslo, Norway

DEVELOPMENT LENGTHS OF LAMINAR FLOW OF SHEAR THINNING FLUIDS IN TUBES

CHRYSO LAMBRIDE,[*] ALEXANDROS SYRAKOS[*] AND GEORGIOS C. GEORGIOU[†]

[*] Department of Mechanical and Manufacturing Engineering
University of Cyprus
PO Box 20537, 1678 Nicosia, Cyprus
e-mail: chrysolambride@hotmail.com , syrakos.alexandros@ucy.ac.cy

[†] Department of Mathematics and Statistics
University of Cyprus
PO Box 20537, 1678 Nicosia, Cyprus
email: georgios@ucy.ac.cy

Key words: Development Length, Shear Thinning Fluid, Wall Shear Stress, Laminar Flow.

Abstract. The development length needed for tube flows to re-adjust from a uniform to the fully-developed velocity profile is usually defined as the length required for the centerline velocity to reach 99% of its fully-developed value. This definition, however, may be quite inaccurate in non-Newtonian flows with almost flat velocity distributions near the centerline, since the velocity far from the axis of symmetry develops more slowly. Shear-thinning and viscoplasticity may cause the flow close to the centerline to evolve faster than that closer to the walls. Thus, alternative definitions of the development length have been proposed for viscoplastic flows. Given that blood exhibits shear thinning, we numerically solve the flow development of power-law fluids in pipes and calculate the development length as a function of the radius, determining the global development length along with the standard centerline estimate. We also consider an alternative definition, based on the evolution of the wall shear stress. Results have been obtained for values of the power-law exponent n ranging from 0.2 to 1 (shear thinning regime) and for Reynolds numbers (Re) up to 1000. The numerical results demonstrated that the centerline and the global development lengths coincide for $n > 0.7$, i.e., the flow indeed develops more slowly at the symmetry axis. This is not the case, however, as the fluid becomes more shear thinning. Big differences are observed, which are more pronounced at low Re. The stress entrance length is smaller than the classical centerline entrance length except for $n < 0.4$. The implications in blood flow development are discussed.

1 INTRODUCTION

When fluid particles flowing with a uniform velocity profile enter a long tube, they are expected to eventually adjust to the fully developed Poiseuille velocity profile far downstream. The required distance is called the development or entrance length. During the development phase, the velocity profile evolves, with the velocity near the walls decelerating due to friction and the velocity near the centre accelerating due to continuity. Knowledge of the development length is important in the design of pipe flow networks and in studies concerned with transition to turbulence [1]. Moreover, it is used in checking the validity of the Poiseuille-flow assumption that is often made in order to simplify calculations of parameters of interest, such as the maximum velocity and the wall shear stress, in flows of industrial importance as well as in flows of biological fluids (biofluids) [2].

Flow development of Newtonian fluids has been extensively studied via approximate analytical, computational, and experimental methods [3]. The standard definition of the development length is the length required for the centerline velocity to reach 99% of its fully developed (Poiseuille) value, starting from a flat velocity profile at the entrance. Different empirical formulas have been proposed relating the development length to the Reynolds number *Re* [3]. Kountouriotis et al. [4] studied the Newtonian flow development in the presence of wall slip, and consider also the "wall development length" as the length required for the slip velocity to decrease to 1.01% of its fully-developed value.

Non-Newtonian flow development is of great interest, since most fluids of industrial and also biological importance can exhibit a variety of complex behaviour such as shear-thinning (or thickening), viscoplasticity, viscoelasticity, and thixotropy. For example, blood exhibits each of the aforementioned rheological phenomena to some degree [5,6]. The non-Newtonian character of blood is predominant in small arteries and veins where the diameter is close to the size of red blood cells [7]. Barnes [8] reports typical shear rate values for blood flow in the range 1-1000 s^{-1}.

It is well established that in the viscoplastic case, the standard definition of the development length is not really representative of the actual length needed for the flow to develop fully ([9,10] and references therein). Recently, Philippou et al. [9] calculated the development length as a function of the radial distance, with and without wall slip, and proposed the "global" development length which is the maximum development length across the tube or channel.

Shear-thinning is a rheological phenomenon that is exhibited by most non-Newtonian fluids, is relatively easy to measure and to model, and in some applications is the only non-Newtonian behaviour that needs to be accounted for in order to get a sufficiently accurate picture of the flow. Shear thinning is considered to be the predominant non-Newtonian characteristic of blood and other biofluids. The decrease of viscosity with the shear rate is attributed to the destruction of rouleaux and the disaggregation of red blood cells (RBCs) which orient themselves in the direction of the flow. For example, Barnes [8] provides data showing that blood viscosity is reduced from 0.1 Pa·s at a shear rate $\dot{\gamma}$=0.1 s^{-1} to 0.01 Pa·s at $\dot{\gamma}$=100 s^{-1}. Many different models describing shear-thinning behavior have been proposed in the literature. As far as blood is concerned, the constitutive equations that have been used include the power-law, Carreau, Carreau-Yasuda, Powell-Eyring, Cross, modified-Cross, Walburn-Schneck, and Ballyk models [11,12].

The power-law model is the simplest non-Newtonian constitutive equation able to describe shear thinning. The viscosity takes the following form [13].

$$\eta = k\dot{\gamma}^{n-1} \tag{1}$$

Table 1: Values of the power-law material parameters used in different studies for blood

Reference	k (Pa s^n)	n
Baaijens [14]	0.028	0.63
Neofytou [15]; Karimi et al. [11]; Mendieta et al. [16]	0.01467	0.7755
Shibeshi and Collins [7]	0.017	0.708
Johnston et al. [17]; Soulis et al. [18]	0.035	0.6
Sequeira and Janela [19]	0.042	0.61
Li et al. [20]	0.035	0.61

where k is the consistency index, n is the power-law exponent, and $\dot{\gamma}$ is the magnitude of the rate of strain tensor, $\dot{\boldsymbol{\gamma}}$, defined by $\dot{\gamma} = \sqrt{\dot{\boldsymbol{\gamma}} : \dot{\boldsymbol{\gamma}}}$. For $n = 1$, the viscosity is constant and the Newtonian model is recovered. The fluid is shear-thinning when n<1 and shear-thickening when n>1. According to Shibeshi and Collins [7], the material parameters k and n are dependent on the constituents of blood, such as hematocrit, fibrinogen and cholesterol, and on temperature. Table 1 lists indicative values used in the literature for these two material parameters. Note, in particular, that the values of n vary from 0.6 to 0.78. Chandran et al. [21] also note that rotational-viscometer data on blood for shear rates in the range from 5 to 200 s^{-1} are satisfactorily fitted with power-law exponents between 0.68 and 0.8.

In most studies of flow development of shear-thinning fluids, the power-law model has been used [1], but other models have also been employed [22]. To our knowledge, in all these studies, the standard definition of the development length has been used, assuming that the centerline/midplane velocity is a sufficient indicator of the flow development. Poole and Ridley [1] showed that at low Reynolds numbers the development length depends on the shear-thinning (or thickening) exponent, similarly to the dependence of the development length of viscoplastic flows on the yield stress. In particular, they found that, in the creeping flow limit, shear thinning causes the development length to increase, up to a shear-thinning exponent of about n=0.4; below this value, further strengthening of the shear-thinning behaviour causes a rapid reduction of the development length, as the fully developed velocity profile becomes more plug-like and similar to the inlet profile, as for the viscoplastic case.

In the present work we investigate whether the standard definition of the development length provides an accurate criterion for the full development of the flow of shear-thinning fluids. The behaviour of shear-thinning fluids is known to be in some respects similar to that of viscoplastic fluids [23]. The stronger the shear-thinning is, the more qualitatively similar (plug-like) the fully developed velocity profile is to the corresponding viscoplastic one. Therefore, monitoring the velocity field only at the centerline may be misleading, as in the viscoplastic case. Our study investigates numerically the development of the flow of power-law fluids for exponents n ranging between 0.2 and 1 (shear thinning regime) and Reynolds numbers up to 1000.

In addition to the standard centerline and global development lengths, which are based on the evolution of the velocity, we introduce an alternative definition based on the evolution of the wall shear stress: it is the length after which the wall shear stress lies between 0.99 and 1.01 times its fully-developed value. In many applications, including blood flows, the wall shear stress is more crucial than the velocity – for example, blood vessels are lined with endothelial cells, whose growth, remodelling and function can be modified by the flow stresses [24].

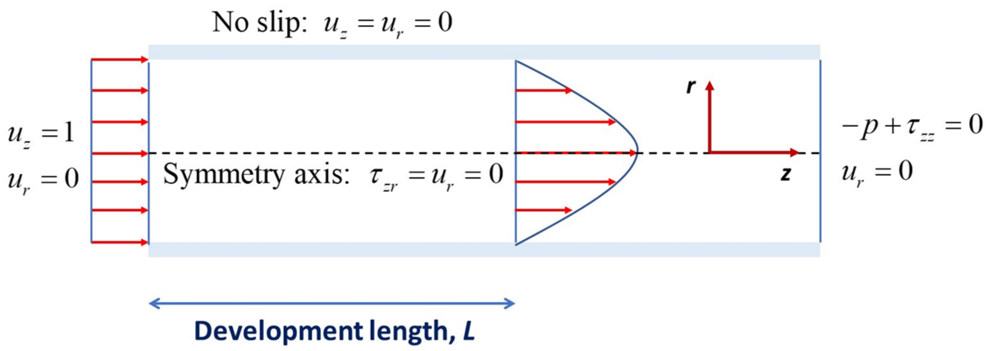

Figure 1: Flow development in a cylindrical tube: geometry and boundary conditions

2 GOVERNING EQUATIONS AND NUMERICAL METHOD

We consider the entrance flow of a shear thinning fluid in a long cylindrical tube of radius R and length L, where the fluid enters with a uniform velocity U. It is assumed that the fluid obeys the power-law constitutive equation [13], whose tensorial form is as follows:

$$\boldsymbol{\tau} = k\dot{\gamma}^{n-1}\dot{\boldsymbol{\gamma}} \tag{2}$$

where $\boldsymbol{\tau}$ is the viscous stress tensor. It is also assumed that the flow is steady, incompressible, and isothermal. The continuity and momentum equations governing the flow then read:

$$\nabla \cdot \mathbf{u} = 0 \tag{3}$$

and

$$\rho \mathbf{u} \cdot \nabla \mathbf{u} = -\nabla p + \nabla \cdot \boldsymbol{\tau} \tag{4}$$

where $\boldsymbol{u}$ and p are the velocity and pressure fields, respectively, and ρ is the constant density. We non-dimensionalize the physical flow problem by scaling lengths by the tube radius R, the velocity by the uniform velocity U at the inlet of the tube, $\dot{\boldsymbol{\gamma}}$ by U/R, and the stress tensor and the pressure by $k\,U^n/R^n$. For the sake of simplicity, we keep the same symbols for the dimensionless variables. Therefore, the dimensionless continuity equation is the same as Eq. (3), while the constitutive and momentum equations become

$$\boldsymbol{\tau} = \dot{\gamma}^{n-1}\dot{\boldsymbol{\gamma}} \tag{5}$$

and

$$Re\,\mathbf{u} \cdot \nabla \mathbf{u} = -\nabla p + \nabla \cdot \boldsymbol{\tau} \tag{6}$$

where

$$Re = \frac{\rho U^{2-n} R^n}{k} \tag{7}$$

is the Reynolds number.

The flow geometry and the boundary conditions are illustrated in Fig. 1. Cylindrical coordinates centered at the symmetry axis of the tube constitute the natural choice for the coordinate system. At the wall ($r = 1$) the no-slip, no-penetration conditions are applied and thus both the axial and radial velocity components, u_z and u_r, vanish. The usual symmetry conditions are applied at the symmetry axis ($r = 0$). At the inflow plane ($z = 0$), the axial velocity is uniform ($u_z = 1$), while u_r is zero. Finally, the outflow plane is taken sufficiently far downstream so that the length of the domain, L_{mesh}, is much longer than the calculated development lengths. In this case, the normal stress and radial velocity components are essentially zero.

The system of the z- and r-components of the momentum equation and the continuity equation is solved using the finite element method [4]. The Newton method is used in solving iteratively the resulting non-linear system of the discretized equations and the convergence tolerance has been set to 10^{-4}.

3 NUMERICAL RESULTS

We have obtained results for power-law exponents ranging from 0.2 to 1 (Newtonian fluid) and for Reynolds numbers from zero up to 1000. The convergence of the numerical results has been confirmed using meshes of different refinement and different lengths. All the results presented below have been obtained with a rather long mesh with L_{mesh}=1120, which was found to be adequately long for the highest value of the Reynolds number considered here. The distribution of the development length across the pipe, $L(r)$ has been calculated by determining the distance beyond which the velocity for a given value of r lied between 0.99-1.01 times its fully developed value. Thus, the standard centerline development length is simply $L_c = L(0)$ and the global development length is $L_g = \max_{0 \le r \le 1} L(r)$. We have also calculated the wall shear stress development length, L_t. To facilitate comparisons with the literature, the development lengths are scaled by the diameter of the tube. However, all other length quantities are scaled by the radius and the Reynolds number is expressed in terms of the radius too; see Eq. (6).

The distribution of the development length $L(r)$ at zero Reynolds number is illustrated in Fig. 2 for $n = 1$ (Newtonian fluid) and $n = 0.3$. One observes that the centerline and global development lengths coincide in the former case, which implies that the flow readjustment is indeed slower at the centerline. This is not the case for low values of the power-law exponent, as in Fig. 2b. This is somehow expected since the velocity profile becomes more flattened as the power-law exponent is reduced. Indeed, the fully-developed dimensionless velocity distribution is given by [13]:

$$u_z = \frac{3n+1}{n+1}\left(1 - r^{1/n+1}\right) \tag{8}$$

Hence, the velocity tends asymptotically to a flat profile as n approaches zero. The maximum (centerline) velocity takes the values 2 and 1.4615 for $n = 1$ and $n = 0.3$, respectively. The development of the velocity for these two values of the power-law exponent is illustrated in Fig. 3, where the distributions of the axial velocity at different distances from the inlet plane are plotted. As the power-law exponent is reduced, the fluid particles at the symmetry axis have to travel a shorter distance in order to accelerate up to the fully-developed maximum velocity.

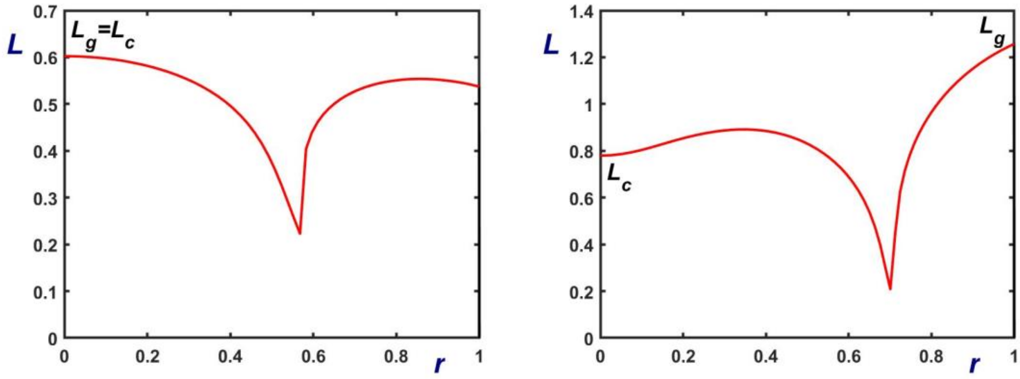

(a) (b)

Figure 2: Distribution of the development length, $L(r)$, in axisymmetric flow of a power-law fluid at $Re = 0$: (a) $n = 1$ (Newtonian fluid, the centreline and global development lengths coincide); (b) $n = 0.3$

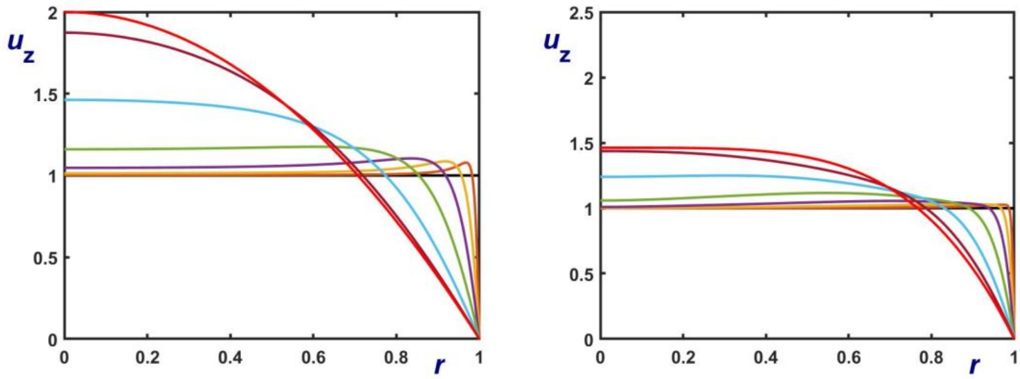

(a) (b)

Figure 3: Velocity profiles at $z = 0$, 0.02, 0.05, 0.1, 0.2, 0.40, 0.81 and 20 in axisymmetric flow development of a power-fluid at $Re = 0$: (a) $n = 1$ (Newtonian fluid); (b) $n = 0.3$

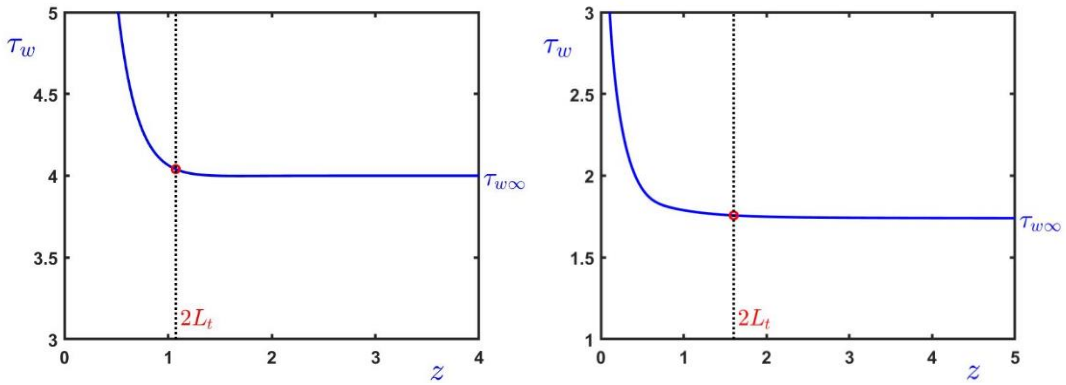

(a) (b)

Figure 4: Wall shear stress distributions in axisymmetric flow development of a power-law fluid at $Re = 0$: (a) $n = 1$ (Newtonian fluid); (b) $n = 0.3$. The vertical line denotes the stress development length, $2L_t$

Figure 4 shows the distribution of the wall shear stress and the corresponding stress development lengths at zero Reynolds number for $n = 1$ and 0.3. Given that L_t is scaled by the diameter and z by the radius of the pipe, the former is multiplied by a factor of 2. Due to the sudden change in the velocity at the inlet plane (the velocity changes abruptly from unity to zero when the fluid particles hit the wall), the wall shear stress, defined by

$$\tau_w = \left|\tau_{rz}\right|_{r=1} = \left(\frac{du_z}{dr}\right)^n \bigg|_{r=1} \tag{9}$$

is singular. Initially it becomes infinite and then converges, not necessarily monotonically (in some cases undershoots are observed), to the fully-developed value

$$\tau_{w\infty} = \left(3 + \frac{1}{n}\right)^n \tag{10}$$

We observe that L_t increases with shear thinning, as the wall shear stress needs to adjust to a lower fully-developed value ($\tau_{w\infty} = 4$ for $n = 1$ and $\tau_{w\infty} = 1.74$ for $n = 0.3$).

In most flow development studies, the nondimensional development length is expressed as a function of the Reynolds number [3]. The effects of the power-law exponent and the Reynolds number on the three development lengths considered in this work are illustrated in Figs. 5 and 6. In Fig. 5, the development lengths are plotted versus the power-law exponent for $Re = 0$, 10 and 100. We observe that L_g and L_c essentially coincide for $n > 0.7$. Below this value, L_g is higher than L_c. The difference between these two lengths becomes more pronounced at lower values of n and Re, which implies that the flow is not fully developed at a distance equal to the standard development length. While L_g is a decreasing function of the power-law exponent, the behavior of L_c is non-monotonic. The standard development length appears to initially increase with the power-law exponent, exhibiting a maximum after which it decreases merging eventually with L_g. The stress development length appears to be smaller than the other two lengths at moderate and high Reynolds numbers and the differences become bigger as the power-law exponent is reduced. At low values of the Reynolds numbers, however, L_t becomes bigger than L_c in the regime where the latter is an increasing function of the power-law exponent (Fig. 5a).

The variation of the development lengths with the Reynolds number in the range 0-1000 is illustrated in Fig. 6 for $n = 1$ and 0.5. In Newtonian flow ($n = 1$), centerline and global development lengths coincide while the stress development length is smaller, especially at low values of the Reynolds number. The difference of L_t from the other development lengths is reduced as Re is increased and the three curves eventually merge for $Re > 20$. The situation changes with shear thinning fluids. As illustrated in Fig. 6b, when $n = 0.5$, $L_t < L_c < L_g$. The difference between L_g and L_c is more pronounced at low values of Re ($Re < 10$) and reduces as Re is increased. The difference between L_t and L_c is small, especially at low Reynolds numbers.

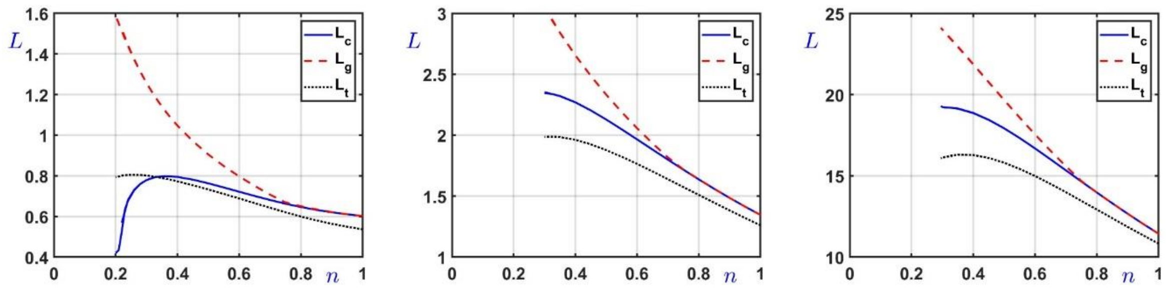

(a) **(b)** **(c)**

Figure 5: Variation of the centerline (L_c), global (L_g), and stress (L_t) development lengths with the power-law exponent: (a) $Re = 0$; (b) $Re = 10$; (c) $Re = 100$

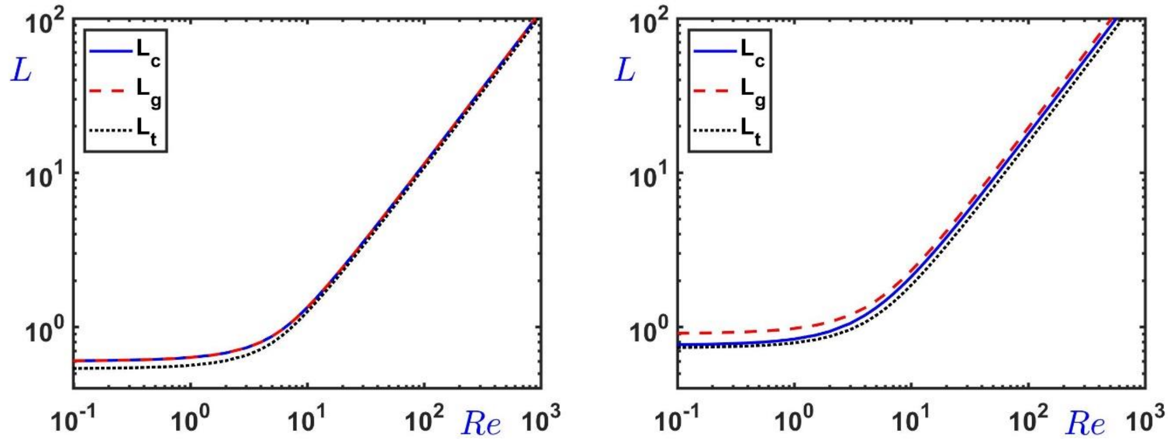

(a) **(b)**

Figure 6: Variation of the centerline (L_c), global (L_g), and stress (L_t) development lengths with the Reynolds number: (a) $n = 1$ (Newtonian fluid); (b) $n = 0.5$

4 CONCLUSIONS

It has been demonstrated that the stress development length in a cylindrical tube is always shorter than the centerline development length, except when $n < 0.4$ and the Reynolds number is low. The use of this development length may be more meaningful in other geometries. In their study of Newtonian flow development in the presence of wall slip, Kountouriotis et al. [4] demonstrated that, in channel flow the slip-velocity development length is higher than the centerline one, in contrast to pipe flow. Given that the slip velocity generally increases with wall shear stress [25], it is anticipated that the behavior of the stress development length is quite similar. The investigation of the flow development of a power-law fluid in a channel is the subject of our current research efforts.

In this numerical study, we have investigated the flow development of power-law fluids in an axisymmetric tube. In addition to the standard definition of the development length, L_c, which is based on the centerline velocity, we also considered the global development length,

L_g, defined in terms of the axial velocity distribution, and the stress development length, L_t, based on the development of the wall shear stress. The numerical results for $0.2 < n \leq 1$ and $0 \leq Re \leq 1000$ indicate that the standard development length is a reliable index of flow development for values of the power-law exponent greater than 0.7, independently of the Reynolds number. For more shear-thinning fluids, however, the centerline development length is misleading, since the flow develops more slowly far from the symmetry axis. The relative differences are more striking at low Reynolds numbers at which L_g can be four times L_c. Hence, attention must be paid when using the assumption of fully developed flow for shear thinning fluids in tubes when the Reynolds number is small, e.g., for flows of blood or other biofluids in small vessels.

REFERENCES

[1] Poole, R. and Ridley, S.B. Development length requirements for fully-developed laminar pipe flow of inelastic non-Newtonian liquids. *ASME J. Fluids Eng.* (2007) **129**:1281-1287.

[2] Clark, A.R., Lin, M., Tawhai, M., Saghian, R., and James, J.L. Multiscale modelling of the feto–placental vasculature. *Interface Focus* (2015) **5**:20140078.

[3] Durst, F., Ray, S., Unsal, B., and Bayoumi, O.A. The development lengths of laminar pipe and channel flows. *ASME J. Fluids Eng.* (2005) **127**:1154-1160.

[4] Kountouriotis, Z., Philippou, M., and Georgiou, G.C. Development lengths in Newtonian Poiseuille flows with wall slip. *Appl. Math. Comp.* (2016) **291**:98-114.

[5] Vlastos, G., Lerche, D., and Koch, B. The superposition of steady on oscillatory shear and its effect on the viscoelasticity of human blood and a blood-like model fluid. *Biorheology* (1997) **34**:19–36.

[6] Armstrong, M., Horner, J., Clark, M., Deegan, M., Hill, T., Keith, C., and Mooradian, L. Evaluating rheological models for human blood using steady state, transient, and oscillatory shear predictions. *Rheol. Acta* (2018) **57**:705-728.

[7] Shibeshi, S.S., and Collins, W.E. The rheology of blood flow in a branched arterial system. Applied Rheology (2005) **15**:398-405.

[8] Barnes, H.A. *A Handbook of Elementary Rheology*. University of Wales (2000)

[9] Philippou, M., Kountouriotis, Z., and Georgiou, G.C. Viscoplastic flow development in tubes and channels with wall slip. *J. non-Newtonian Fluid Mech.* (2016) **234**:69-81.

[10] Panaseti, P., and Georgiou, G.C. Viscoplastic flow development in a channel with slip along one wall. J. non-Newtonian Fluid Mech. (2017) **248**:8-22.

[11] Karimi, S., Dabagh, M., Vasana, P., Dadvar, M., Dabir, B., and Jalali, P. Effect of rheological models on the hemodynamics within human aorta: CFD study on CT image-based geometry. *J. non-Newtonian Fluid Mech.* (2014) **207**:42-52.

[12] Kannojiya, V., Das, A.K., and Das, P.K. Simulation of blood as fluid: A review from rheological aspects. *IEEE Rev. Biomed. Engin.* (2020) **14**:327-341.

[13] Bird, R.B., Curtiss, C.F., Armstrong, R.C., and Hassager, O. *Dynamics of Polymeric Liquids, Vol. 1, Fluid Mechanics*, 2nd edn. Wiley, New York (1987).

[14] Baaijens, J.P.W. *A literature research into the rheology of human blood*. WFW-Report no. WFW-90,065. Eindhoven University of Technology (1991).

[15] Neofytou, P. Comparison of blood rheological models for physiological flow simulation. *Biorheology* (2004) **41**:693-714.
[16] Mendieta, J.B., Fontanarosa, D., Wang, J., Paritala, P.K., McGahan, T., Lloyd, T., Li, Z. The importance of blood rheology in patient-specific computational fluid dynamics simulation of stenotic carotid arteries. *Biomech. Model. Mechanobiology* (2020) **19**:1477-1490.
[17] Johnston, B.M., Johnston, P.R., Corney, S., and Kilpatrick, D. Non-Newtonian blood flow in human right coronary arteries: steady state simulations. *J. Biomechanics* (2004) **37**: 709-720.
[18] Soulis, J.V., Giannoglou, G.D., Chatzizisis, Y.S., Seralidou, K.V., Parcharidis, G.E., and Louridas, G.E. Non-Newtonian models for molecular viscosity and wall shear stress in a 3D reconstructed human left coronary artery. *Med. Eng. Phys.* (2008) **30**:9-19.
[19] Sequeira, A., and Janela, J. An overview of some mathematical models of blood rheology. In Seabra Pereira, M. (Ed.) *A portrait of state-of-the-art research at Technical University of Lisbon*. Springer (2007):65-87.
[20] Li, X.-W., Wen, G.-B., and Li, D. Computer simulation of non-Newtonian flow and mass transport through coronary arterial stenosis. *Appl. Maths. Mech.* (2001) **22**:409-424.
[21] Chandran, K.B., Yoganathan, A.P., and Rittgers, S.E. *Biofluid Mechanics: the Human Circulation*. CRC Press, Boca Raton (2007).
[22] Fernandes, C., Ferrás, L.L., Araujo, M.S., and Nóbrega, J.M. Development length in planar channel flows of inelastic non-Newtonian fluids. *J. non-Newtonian Fluid Mech.* (2018) **255**:13-18.
[23] Syrakos, A., Dimakopoulos, Y., and Tsamopoulos, J. A finite volume method for the simulation of elastoviscoplastic flows and its application to the lid-driven cavity case. *J. non-Newtonian Fluid Mech.* (2020) **275**:104216.
[24] Grotberg, J.B. *Biofluid Mechanics: Analysis and Applications*. Cambridge University Press (2021).
[25] Panaseti, P., Housiadas, K.D., and Georgiou, G.C. Newtonian Poiseuille flows with pressure-dependent slip. *J. Rheology* (2013) **57**:315-332.